

A Dirac fermion model associated with second order topological insulator

Takahiro Fukui

Department of Physics, Ibaraki University, Mito 310-8512, Japan

(Dated: March 19, 2019)

We study topological aspects of a Dirac fermion coupled with a Higgs field associated with the lattice model introduced by Benalcazar *et al.* which has the topological quadrupole phase. Using the index theorem, we show that the index of the Hamiltonian is just given by the winding number of the Higgs field, implying that a corner state of the lattice model belongs to the same class of the Jackiw-Rossi states localized at a vortex. We also calculate the current density of the Dirac fermion with a symmetry breaking term dependent on time, which is associated with the dipole pump proposed by Benalcazar *et al.*. We argue that it is indeed a topological current, and the total pumped charge is given by an integer related with the index.

I. INTRODUCTION

The bulk-edge correspondence is one of key properties which characterizes topological phases of matter. While it has been established for the quantum Hall system [1], the discovery of the quantum spin Hall effect and more generic topological insulators [2–6] has revealed that the bulk-edge correspondence is valid for wider classes of topological phases. Weyl semimetals also show unique edge (surface) states called Fermi-arc [7–9], which reflect the topological property of the bulk system such as section Chern numbers.

Recently, further development has been achieved by Benalcazar, *et al.* [10, 11]. They have proposed higher order topological insulators which are characterized by $d-D$ dimensional edge (surface) states for d dimensional bulk systems. Conventional topological insulators correspond to $D = 1$, but nontrivial systems with $D > 1$ have been successively found and studied extensively [12–25]. In particular, Khalaf [21] has pointed out that the corner can be regarded as a topological defect and has given the classification table of the higher-order topological insulators and superconductors protected by inversion symmetry, and Trifunovic and Brouwer [24] have extended the table considering generic order-two crystalline (anti)-symmetries. The corner states in $d = D = 2$ dimensional system have indeed observed experimentally in metamaterial circuit systems [20].

In this paper, we study a Dirac fermion model associated with the lattice Benalcazar-Bernevig-Hughes (BBH) model [10, 11]. As the two-dimensional BBH model shows zero-dimensional corner states, it is a second order topological insulator with $D = 2$. Although the lattice BBH model includes four Dirac fermions, we pick up one of them and examine the topological properties of the single Dirac fermion.

In the next section, we will take the continuum limit of the BBH model. Regarding the BBH model as a generalized Wilson-Dirac model [26], we point out that we need not only the Dirac fermion at $\mathbf{k} = (0, 0)$, but also its doublers at $\mathbf{k} = (\pi, 0), (0, \pi), (\pi, \pi)$. These fermion models have the same structure: a Dirac fermion model coupled with an O(2) Higgs field, belonging to the sym-

metry class BDI [27, 28], so we examine the topological property of such a single Dirac fermion. We show that this model indeed needs corner-like boundaries to have zero energy states. In Sec. III, we discuss the topological property of such corner states using the index theorem. To this end, we introduce smooth boundaries as a smoothly-varying Higgs field as a function of the coordinates. It then turns out that since a corner can be regarded as a point defect, a corner state belongs to the same class of the Jackiw-Rossi states localized at a vortex [29]. Therefore, the present model belongs to class BDI with a point defect in the classification table given by Teo and Kane [30]. In Sec. IV, introducing a symmetry breaking term dependent on time, we consider a pump of the present Dirac model which corresponds to the dipole pump proposed by BBH [10, 11]. We calculate the current density for a model with a single defect (a smooth corner as in Sec. III). It is shown that the current is indeed topological, and the total pumped charge is given by an integer associated with the index derived in Sec. III. When we argue the topological phases of the lattice model, we need to take all Dirac fermions including doublers into account. We will discuss the problem in Sec. V. In Appendix A, we will give a similar formulation for the one-dimensional Su-Schrieffer-Heeger (SSH) model [31], which may be helpful in understanding the relationship between the continuum Dirac fermions and the phase of the BBH (or SSH) lattice model.

II. DIRAC FERMION MODEL

In this section, we first introduce the BBH lattice model, and next, take the continuum limit. The Dirac fermion model thus obtained belongs to class BDI [27, 28], and boundary zero energy states can be easily obtained.

The BBH model introduced in [10, 11] is a two-dimensional version of the SSH model [31]. The BBH Hamiltonian is defined explicitly by

$$H(\mathbf{k}) = \Gamma^j g_j(\mathbf{k}), \quad (1)$$

where $g_j(k)$ is given by

$$\begin{aligned} g_1 &= \lambda_x \sin k_x \\ g_2 &= \lambda_y \sin k_y \\ g_3 &= \gamma_x + \lambda_x \cos k_x \\ g_4 &= \gamma_y + \lambda_y \cos k_y. \end{aligned} \quad (2)$$

Here, γ_j is the hopping within a unit cell, whereas λ_j is the hopping between the unit cells in the $j = x, y$ direction. Benalcazar *et al.* have chosen the Γ -matrices such that $\Gamma^1 = -\sigma^3 \otimes \sigma^2$, $\Gamma^2 = -\sigma^1 \otimes \sigma^2$, $\Gamma^3 = 1 \otimes \sigma^1$, and $\Gamma^4 = -\sigma^2 \otimes \sigma^2$ as well as $\Gamma_5 = -1 \otimes \sigma^3$, but any other definitions may be possible if they obey $\{\Gamma^j, \Gamma^l\} = 2\delta^{jl}$ ($j, l = 1, \dots, 4$) and $\Gamma_5 = (-i)^2 \Gamma^1 \Gamma^2 \Gamma^3 \Gamma^4$, so that $\text{tr} \Gamma_5 \Gamma^1 \Gamma^2 \Gamma^3 \Gamma^4 = (2i)^2$.

A. Continuum limit of the BBH model

The lattice model (2) includes four Dirac fermions at $k_j = 0, \pi$.

$$\begin{aligned} H_{(0,0)} &= +\Gamma^1 \lambda_x k_1 + \Gamma^2 \lambda_y k_2 + \Gamma^3 (\gamma_x + \lambda_x) + \Gamma^4 (\gamma_y + \lambda_y), \\ H_{(\pi,0)} &= -\Gamma^1 \lambda_x k_1 + \Gamma^2 \lambda_y k_2 + \Gamma^3 (\gamma_x - \lambda_x) + \Gamma^4 (\gamma_y + \lambda_y), \\ H_{(0,\pi)} &= +\Gamma^1 \lambda_x k_1 - \Gamma^2 \lambda_y k_2 + \Gamma^3 (\gamma_x + \lambda_x) + \Gamma^4 (\gamma_y - \lambda_y), \\ H_{(\pi,\pi)} &= -\Gamma^1 \lambda_x k_1 - \Gamma^2 \lambda_y k_2 + \Gamma^3 (\gamma_x - \lambda_x) + \Gamma^4 (\gamma_y - \lambda_y). \end{aligned} \quad (3)$$

As we will argue in Sec. V, we need to consider all the contributions from these Dirac fermions to clarify the topological property of the lattice BBH model. However, for the time being, we consider a single Dirac fermion of the form,

$$H(\mathbf{k}) = \Gamma^j k_j + \Gamma^{a+2} \phi_a, \quad (4)$$

where $j = 1, 2$ ($x^1 = x, x^2 = y$), $a = 1, 2$. This is a model of the two-dimensional Dirac fermion coupled with a $O(2)$ Higgs field $\phi = (\phi_1, \phi_2)$, belonging to class BDI with time-reversal, particle-hole, and chiral symmetries denoted, respectively, by

$$\begin{aligned} TH(\mathbf{k})T^{-1} &= H(-\mathbf{k}), \\ CH(\mathbf{k})C^{-1} &= -H(-\mathbf{k}), \\ \Gamma_5 H(\mathbf{k})\Gamma_5^{-1} &= -H(\mathbf{k}), \end{aligned} \quad (5)$$

where $T = K$ (taking complex conjugate) and $C = \Gamma_5 K$. In addition to these, this Hamiltonian has reflection symmetries.

$$\begin{aligned} M_x H(k_x, k_y) M_x^{-1} &= H(-k_x, k_y), \\ M_y H(k_x, k_y) M_y^{-1} &= H(k_x, -k_y), \end{aligned} \quad (6)$$

where $M_x = i\Gamma^1 \Gamma_5$ and $M_y = i\Gamma^2 \Gamma_5$.

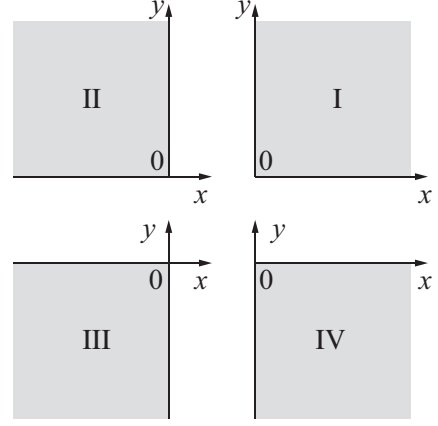


FIG. 1: Four types of corners.

B. Boundary zero energy states

The energy eigenvalues of the Hamiltonian (4) are gapped at the zero energy, given by $E = \pm \sqrt{\sin^2 k_j + \phi_j^2}$. However, if the system has boundaries, the model allows zero energy states, $H\psi = 0$. The Hamiltonian in the coordinate representation is given by

$$\begin{aligned} H &= \begin{pmatrix} & D^\dagger \\ D & \end{pmatrix}, \\ D &= -\sigma^3 \partial_x - \sigma^1 \partial_y - i\sigma^2 \phi_y + \phi_x \\ &= \begin{pmatrix} -\partial_x + \phi_x & -\partial_y - \phi_y \\ -\partial_y + \phi_y & \partial_x + \phi_x \end{pmatrix}. \end{aligned} \quad (7)$$

For simplicity, we here assume ϕ_x and ϕ_y are positive constants, $\phi_x, \phi_y > 0$. Let us set $\psi = (\xi, \eta)^T$, where ξ and η is the wave function with chirality $\Gamma_5 = -1$ and 1 , respectively. Then, the zero energy equation reads

$$D\xi = 0, \quad D^\dagger \eta = 0, \quad (8)$$

We readily obtain the following normalizable solution depending on the boundaries:

$$\xi_{\text{I}} = \mathcal{N} \begin{pmatrix} 0 \\ e^{-\phi_x x - \phi_y y} \end{pmatrix}, \eta_{\text{I}} = 0, \quad (x > 0, y > 0) \quad (9)$$

$$\xi_{\text{III}} = \mathcal{N} \begin{pmatrix} e^{\phi_x x + \phi_y y} \\ 0 \end{pmatrix}, \eta_{\text{III}} = 0, \quad (x < 0, y < 0) \quad (10)$$

$$\xi_{\text{II}} = 0, \eta_{\text{II}} = \mathcal{N} \begin{pmatrix} e^{\phi_x x - \phi_y y} \\ 0 \end{pmatrix}, \quad (x < 0, y > 0) \quad (11)$$

$$\xi_{\text{IV}} = 0, \eta_{\text{IV}} = \mathcal{N} \begin{pmatrix} 0 \\ e^{-\phi_x x + \phi_y y} \end{pmatrix}, \quad (x > 0, y < 0) \quad (12)$$

where the normalization constant $\mathcal{N} = 2\sqrt{\phi_x \phi_y}$. In the limit $\phi_x, \phi_y \rightarrow +\infty$, the above wave functions become ξ^2 or $\eta^2 \rightarrow \delta(x)\delta(y)$, localized at the origin. Thus, it turns out that the present model allows corner states rather than conventional edge states. See Appendix J in [11].

C. Symmetry-breaking perturbations

So far we have derived the Dirac Hamiltonians of the type (4) and its corner states Eqs. (9)-(12). It turns out that the two independent mass terms protected by reflection symmetries are responsible for the corner states. However, reflection symmetries allow another mass term given by

$$H_{\text{sb}} = i\Gamma^3\Gamma^4\phi_{12}, \quad (13)$$

which has broken chiral and time reversal symmetries (but unbroken particle-hole symmetry). Therefore, if we require auxiliary time reversal symmetry in Eq. (5) as well as reflection symmetries Eq. (6), the Dirac Hamiltonian (4) has inevitably chiral symmetry. This is similar to the SSH Dirac model (A23), in which one of symmetries, e.g., inversion symmetry results in time reversal, chiral symmetries, etc. Such symmetry properties may be due to the fact that the Dirac models (4) and (A23) are minimal models with a corner state and an edge state, respectively.

In the next section, we will investigate the topological properties of the edge states without the mass term (13). It will also turn out that even with Eq. (13), the corner state is still protected by particle-hole symmetry, as will be presented in Sec. V.

Another simple way to break chiral symmetry (as well as particle-hole symmetry) is to extend the model to the layer systems. In Appendix A3, we will demonstrate a similar extension of the SSH model to ladder models. We will show that although the lattice model does not have chiral symmetry, the Dirac fermions with chiral symmetry are responsible for the existence of the edge states and hence the index theorem is a useful tool to investigate them. Even for the present BBH model, such an argument can also be applied, since the Hamiltonian of a layered BBH model is obtained by replacing H_{SSH} and H'_{SSH} with H_{BBH} and H'_{BBH} in Eq. (A21). This implies that the Dirac fermion (4) is the basic effective model describing the corner states. In particular, the corner states of the trilayer system, which has broken chiral symmetry, can be described by the Dirac fermion (4) near half-filling.

III. INDEX THEOREM

The corner states has a topological origin which is the same as the Jackiw-Rossi states localized at a point defect (vortex) given by $\phi = \Delta(r)(\cos\theta, \sin\theta)$ [29]. To see this, we will consider smooth boundaries introduced by a coordinate-dependent Higgs field such that

$$\phi_1 = \phi_x(\mathbf{x}), \quad \phi_2 = \phi_y(\mathbf{y}), \quad (14)$$

where ϕ_x and ϕ_y depends generically on \mathbf{x} with the asymptotic form $\phi_x(x \rightarrow \pm\infty, y) \rightarrow \text{const.}$ and $\phi_y(x, y \rightarrow \pm\infty) \rightarrow \text{const.}$ respectively. For such a model,

we will apply the index theorem on open spaces [32–36]. We assume that the dependence of ϕ_j on x^j is so smooth that $|\partial_j\phi_j| \ll |\phi_j|$ is valid, implying that we can make use of the derivative expansion in the following calculations.

Since the model has chiral symmetry, the zero energy states can be labeled by the chirality. Therefore, let us define the index of H such that

$$\begin{aligned} \text{ind } H &= n_+ - n_- \\ &= \lim_{m \rightarrow 0} \text{Tr } \Gamma_5 \frac{m^2}{H^2 + m^2}, \end{aligned} \quad (15)$$

where n_{\pm} stands for the number of zero energy states with chirality ± 1 . As we will show below, the rhs of the above index can be expressed by the axial vector current

$$\langle j_5^j(\mathbf{x}) \rangle = \lim_{\mathbf{y} \rightarrow \mathbf{x}} \text{tr } \Gamma_5 \Gamma^j \left(\frac{1}{iH + m} - \frac{1}{iH + M} \right) \delta(\mathbf{x} - \mathbf{y}), \quad (16)$$

where the second term with M is a Pauli-Villars regulator. In the following calculation, the regulator will be suppressed. The divergence of the current yields

$$\begin{aligned} \partial_j \langle j_5^j \rangle &= \partial_j^x \lim_{\mathbf{y} \rightarrow \mathbf{x}} \text{tr } \Gamma_5 \Gamma^j \frac{1}{iH + m} \delta(\mathbf{x} - \mathbf{y}) \\ &= \lim_{\mathbf{y} \rightarrow \mathbf{x}} \text{tr } \Gamma_5 \Gamma^j (\partial_j^x + \partial_j^y) \frac{1}{iH + m} \delta(\mathbf{x} - \mathbf{y}) \\ &= \lim_{\mathbf{y} \rightarrow \mathbf{x}} \text{tr } \Gamma_5 \left(\Gamma^j \partial_j^x \frac{1}{iH + m} + \frac{1}{iH + m} \Gamma^j \partial_j^x \right) \delta(\mathbf{x} - \mathbf{y}). \end{aligned} \quad (17)$$

Here, note that $iH = \Gamma^j \partial_j + i\Gamma^{a+2}\phi_a$, and the Higgs term anti-commutes with Γ_5 . Then, we have

$$\begin{aligned} \partial_j \langle j_5^j \rangle &= \lim_{\mathbf{y} \rightarrow \mathbf{x}} \text{tr } \Gamma_5 (2iH) \frac{1}{iH + m} \delta(\mathbf{x} - \mathbf{y}) \\ &= 2 \lim_{\mathbf{y} \rightarrow \mathbf{x}} \text{tr } \Gamma_5 \left(1 - \frac{m}{iH + m} \right) \delta(\mathbf{x} - \mathbf{y}) \end{aligned} \quad (18)$$

The term 1 in the parentheses cancels the same one in the regulator. Thus, we have

$$\partial_j \langle j_5^j \rangle = -2 \lim_{\mathbf{y} \rightarrow \mathbf{x}} \text{tr } \Gamma_5 \frac{m(-iH + m)}{H^2 + m^2} \delta(\mathbf{x} - \mathbf{y}). \quad (19)$$

Since H anti-commutes with Γ_5 , we reach

$$\begin{aligned} \partial_j \langle j_5^j \rangle &= -2 \lim_{\mathbf{y} \rightarrow \mathbf{x}} \text{tr } \Gamma_5 \frac{m^2}{H^2 + m^2} \delta(\mathbf{x} - \mathbf{y}) \\ &\quad + 2 \lim_{\mathbf{y} \rightarrow \mathbf{x}} \text{tr } \Gamma_5 \frac{M^2}{H^2 + M^2} \delta(\mathbf{x} - \mathbf{y}), \end{aligned} \quad (20)$$

where we have explicitly denoted the contribution from the regulator. Thus, integrating over the space and taking the limit $m \rightarrow 0$ and $M \rightarrow \infty$ yields

$$\begin{aligned} \text{ind } H &= -\frac{1}{2} \int \partial_j \langle j_5^j \rangle d^2x + c_1 \\ &= -\frac{1}{2} \oint_C \epsilon_{jl} \langle j_5^j \rangle dx^l + c_1, \end{aligned} \quad (21)$$

where C is the contour denoted in Fig. 2, and

$$c_1 = \lim_{M \rightarrow \infty} \text{Tr} \Gamma_5 \frac{M^2}{H^2 + M^2}, \quad (22)$$

is associated with the chiral anomaly. Although this vanishes trivially in the present case with no gauge potentials, it plays an important role in the reproduction of the correct index for the Jackiw-Rossi model in a magnetic field [33, 37].

Let us now compute the current in the derivative expansion:

$$\begin{aligned} \langle j_5^j(\mathbf{x}) \rangle &= \lim_{\mathbf{y} \rightarrow \mathbf{x}} \text{tr} \Gamma_5 \Gamma^j \frac{1}{iH + m} \delta(\mathbf{x} - \mathbf{y}) \\ &= \lim_{\mathbf{y} \rightarrow \mathbf{x}} \int \frac{d^2 k}{(2\pi)^2} \text{tr} \Gamma_5 \Gamma^j \frac{1}{iH + m} e^{i\mathbf{k} \cdot (\mathbf{x} - \mathbf{y})} \\ &= \int \frac{d^2 k}{(2\pi)^2} \text{tr} \Gamma_5 \Gamma^j e^{-i\mathbf{k} \cdot \mathbf{x}} \frac{-iH + m}{H^2 + m^2} e^{i\mathbf{k} \cdot \mathbf{x}}, \quad (23) \end{aligned}$$

where the Pauli-Villars regulator has been suppressed. Note here that

$$\begin{aligned} e^{-i\mathbf{k} \cdot \mathbf{x}} H e^{i\mathbf{k} \cdot \mathbf{x}} &= \Gamma^j k_j + \Gamma^{a+2} \phi_a + O_1, \\ e^{-i\mathbf{k} \cdot \mathbf{x}} H^2 e^{i\mathbf{k} \cdot \mathbf{x}} &= \mathbf{k}^2 + \phi^2 - i\Gamma^j \Gamma^{a+2} \partial_j \phi_a + O_2, \quad (24) \end{aligned}$$

where $\phi^2 = \phi_a^2$, $O_1 = -i\Gamma^\mu \partial_\mu$, and $O_2 = -2ik^\mu \partial_\mu - \partial_\mu^2$.

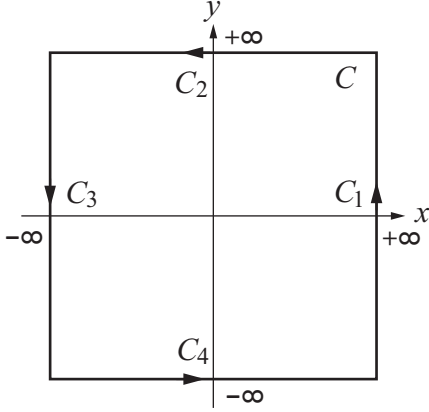


FIG. 2: The integration contour C of $\langle j_5^j(x) \rangle$ in Eq. (21). The closed path C is divided into four lines denoted by C_j ($j = 1, \dots, 4$).

The contour integration in Eq. (21) can be carried out by dividing the path C into four lines C_j . To compute the integration on the line C_1 , let us consider the limit $x \rightarrow \infty$ and regard $\phi_x = \phi_x(+\infty)$ as a constant. Then, $\langle j_5^1(x) \rangle$ at $x^1 \rightarrow +\infty$ can be calculated as follows:

$$\begin{aligned} \langle j_5^1(x^1 \rightarrow +\infty) \rangle &= \int \frac{d^2 k}{(2\pi)^2} \text{tr} \Gamma_5 \Gamma^1 \\ &\times \frac{-\Gamma^j (\partial_j + ik_j) - i\Gamma^3 \phi_x(\infty) - i\Gamma^4 \phi_2 + O_1}{\mathbf{k}^2 + \phi^2 - i\Gamma^2 \Gamma^4 \partial_2 \phi_2 + O_2}, \quad (25) \end{aligned}$$

where we have safely taken the limit $m \rightarrow 0$, while the regulator has vanished in the limit $M \rightarrow \infty$. Note that in the denominator above we assume $|\partial_2 \phi_2| \ll \phi^2$. Therefore, as the leading contribution, we have

$$\begin{aligned} \langle j_5^1 \rangle &= \int \frac{d^2 k}{(2\pi)^2} \text{tr} \Gamma_5 \Gamma^1 (-i\Gamma^3 \phi_x(\infty)) \frac{i\Gamma^2 \Gamma^4 \partial_2 \phi_2}{(\mathbf{k}^2 + \phi^2)^2} \\ &= \frac{1}{\pi} \frac{\phi_x(\infty) \partial_2 \phi_2}{\phi_x(\infty)^2 + \phi_2^2}. \quad (26) \end{aligned}$$

Thus, the integration on C_1 yields

$$\begin{aligned} \int_{C_1} \langle j_5^1(x) \rangle dy &= \int_{-\infty}^{\infty} \langle j_5^1(x^1 = \infty) \rangle dy \\ &= \frac{1}{\pi} \left[\arctan \frac{\phi_y(\infty)}{\phi_x(\infty)} - \arctan \frac{\phi_y(-\infty)}{\phi_x(\infty)} \right]. \quad (27) \end{aligned}$$

Integration on the other lines C_j can be computed likewise, and we finally reach

$$\begin{aligned}
\int_C \epsilon_{jl} \langle j_5^j \rangle dx^l &= \frac{1}{\pi} \left[\arctan \frac{\phi_y(\infty)}{\phi_x(\infty)} - \arctan \frac{\phi_y(-\infty)}{\phi_x(-\infty)} + \arctan \frac{\phi_x(\infty)}{\phi_y(\infty)} - \arctan \frac{\phi_x(-\infty)}{\phi_y(-\infty)} \right. \\
&\quad \left. - \arctan \frac{\phi_y(\infty)}{\phi_x(-\infty)} + \arctan \frac{\phi_y(-\infty)}{\phi_x(-\infty)} - \arctan \frac{\phi_x(\infty)}{\phi_y(-\infty)} + \arctan \frac{\phi_x(-\infty)}{\phi_y(-\infty)} \right] \\
&= \frac{1}{2} \left[\text{sgn} \frac{\phi_y(\infty)}{\phi_x(\infty)} + \text{sgn} \frac{\phi_y(-\infty)}{\phi_x(-\infty)} - \text{sgn} \frac{\phi_y(-\infty)}{\phi_x(\infty)} - \text{sgn} \frac{\phi_y(\infty)}{\phi_x(-\infty)} \right], \tag{28}
\end{aligned}$$

where we have used the identity $\arctan x + \arctan x^{-1} = \frac{\pi}{2} \text{sgn} x$. It thus turns out that the index is given by

$$\text{ind } H = -\frac{1}{4} \left[\text{sgn} \frac{\phi_y(\infty)}{\phi_x(\infty)} + \text{sgn} \frac{\phi_y(-\infty)}{\phi_x(-\infty)} - \text{sgn} \frac{\phi_y(-\infty)}{\phi_x(\infty)} - \text{sgn} \frac{\phi_y(\infty)}{\phi_x(-\infty)} \right]. \tag{29}$$

This is one of the main results in the present paper. The rhs of the above equation is minus the winding number of $\phi(x) = (\phi_x(x), \phi_y(y))$ around C : If $\phi_x(-\infty) < 0 < \phi_x(+\infty)$, and $\phi_y(-\infty) < 0 < \phi_y(+\infty)$, the winding number equals 1, and the index of H is given by -1 . This configuration of ϕ corresponds to Eq. (9) which has chirality -1 . Other cases in Eqs.(10)-(12) match the index given in Eq. (29). For example, the corner state (11) can be realized by $\phi_x(+\infty) < 0 < \phi_x(-\infty)$ and $\phi_y(-\infty) < 0 < \phi_y(+\infty)$, which has winding number -1 , and hence $\text{ind } H=1$. Therefore, it turns out that a single corner can be regarded as a point defect, and the zero energy state of the BBH Dirac fermion is the same class as the Jackiw-Rossi states localized in a vortex.

In passing, we mention that if the Hamiltonian includes vector and/or axial vector gauge potentials, the boundary integration in Eq. (21) needs careful calculations, constructing the boundary operators and computing their spectral flow [35, 38]. In the present case, however, the model is simple enough to reproduce the index by the simple derivative expansion.

IV. DIPOLE PUMP

Benalcazar *et al.* have proposed a dipole pump and demonstrated it for the BBH model [11]. The continuum Dirac model presented in this paper corresponds to the case with a single corner, which can be realized by a coordinate-dependent Higgs field introduced in the previous section. In this section, we further introduce a symmetry-breaking term dependent on time and calculate the vector current density to investigate a charge pump associated with a corner. Calculations of this section is parallel to those in Ref. [39].

As discussed by BBH, we consider the model which includes symmetry breaking (reflection symmetries, in par-

ticular) term

$$H = -i\Gamma^j \partial_j + \sum_{a=1,2} \Gamma^{a+2} \phi_a + \Gamma_5 \phi_3, \tag{30}$$

where we assume that ϕ_a ($a = 1, 2, 3$) depends not only \mathbf{x} but also t , $\phi_a = \phi_a(t, \mathbf{x})$. For the time being, we only assume that $|\partial_\mu \phi_a| \ll |\phi|$, which allows the derivative expansion. The Lagrangian corresponding to the Hamiltonian (30) is

$$\begin{aligned}
\mathcal{L} &= \bar{\psi}(i\gamma^\mu \partial_\mu - \gamma^3 \phi_1 - \phi_2 - i\gamma_5 \phi_3)\psi \\
&\equiv \bar{\psi}(i\cancel{\partial} - \Phi - \phi_2)\psi, \tag{31}
\end{aligned}$$

where $\mu = 0, 1, 2$ ($x^0 = t$), and γ -matrices obeying $\{\gamma^\mu, \gamma^\nu\} = 2g^{\mu\nu}$ with $g^{\mu\nu} = \text{diag}(1, -1, -1, -1)$ is defined by $\gamma^0 = \Gamma^4$, $\gamma^j = \gamma^0 \Gamma^j$ ($j = 1, 2$), $\gamma^3 = \gamma^0 \Gamma^3$, and $\gamma_5 = i\gamma^0 \gamma^1 \gamma^2 \gamma^3$. The U(1) vector current is defined by

$$\begin{aligned}
\langle j^\mu(x) \rangle &= \langle 0 | \bar{\psi}(x) \gamma^\mu \psi(x) | 0 \rangle \\
&= -\lim_{y \rightarrow x} \langle 0 | T \gamma^\mu \psi(x) \bar{\psi}(y) | 0 \rangle, \tag{32}
\end{aligned}$$

where $x = (t, \mathbf{x})$ and the propagator is given by

$$\langle 0 | T \psi(x) \bar{\psi}(y) | 0 \rangle = \frac{i}{i\cancel{\partial} - \Phi - \phi_2 + i\epsilon} \delta(x - y) \tag{33}$$

In the plane wave representation of the delta function similar to Eq. (23), we have

$$\langle j^\mu(x) \rangle = \int \frac{d^3 k}{i(2\pi)^3} e^{-ikx} \text{tr} \gamma^\mu \frac{1}{i\cancel{\partial} - \Phi - \phi_2 + i\epsilon} e^{ikx}, \tag{34}$$

where $kx = \omega t - \mathbf{k} \cdot \mathbf{x}$. Using

$$\begin{aligned}
&((i\cancel{\partial} - \Phi) - \phi_2) (- (i\cancel{\partial} - \Phi) - \phi_2) \\
&= \partial^2 + \phi^2 + i(\cancel{\partial}\Phi) - i(\cancel{\partial}\phi_2), \tag{35}
\end{aligned}$$

we reach

$$\langle j^\mu(x) \rangle = \int \frac{d^3k}{i(2\pi)^3} \text{tr} \gamma^\mu (-i\cancel{\partial} + \cancel{k} + \Phi - \phi_2) \times \frac{1}{(\partial + ik)^2 + \phi^2 + i(\cancel{\partial}\Phi) - i(\cancel{\partial}\phi_2) - i\epsilon}, \quad (36)$$

where $\phi^2 = \sum_{a=1}^3 \phi_a^2$. Since we assume that the x dependence of $\phi_j(x)$ is so smooth that the derivative expansion is a good approximation, as has done in Sec. III, the leading contribution is

$$\langle j^\mu(x) \rangle = \int \frac{d^3k}{i(2\pi)^3} \text{tr} \gamma^\mu \frac{(\Phi - \phi_2)[i(\cancel{\partial}\Phi) - i(\cancel{\partial}\phi_2)]^2}{(\phi^2 - k^2 - i\epsilon)^3} + O((\partial\phi)^{-3}), \quad (37)$$

where $k^2 = \omega^2 - \mathbf{k}^2$ and $\phi^2 = \sum_{a=1}^3 \phi_a^2$. Note that

$$\begin{aligned} \text{tr} \gamma^\mu (\Phi - \phi_2) [i(\cancel{\partial}\Phi) - i(\cancel{\partial}\phi_2)]^2 &= \text{tr} \gamma^\mu (\gamma^3 \phi_1 + i\gamma_5 \phi_3 - \phi_2) \\ &\times [i\gamma^\nu \gamma^3 \partial_\nu \phi_1 - \gamma^\nu \gamma_5 \partial_\nu \phi_3 - i\gamma^\nu \partial_\nu \phi_2]^2 \\ &= 4\epsilon^{\mu\nu\rho} \epsilon^{abc} \phi_a \partial_\nu \phi_b \partial_\rho \phi_c, \end{aligned} \quad (38)$$

where we have used $\text{tr} \gamma_5 \gamma^\mu \gamma^\nu \gamma^\rho \gamma^\sigma = -4i\epsilon^{\mu\nu\rho\sigma}$. Thus, we reach

$$\begin{aligned} \langle j^\mu(x) \rangle &= 4\epsilon^{\mu\nu\rho} \epsilon^{abc} \phi_a \partial_\nu \phi_b \partial_\rho \phi_c \int \frac{d^3k}{i(2\pi)^3} \frac{1}{(\phi^2 - k^2 - i\epsilon)^3} \\ &= \frac{1}{8\pi\phi^3} \epsilon^{\mu\nu\rho} \epsilon^{abc} \phi_a \partial_\nu \phi_b \partial_\rho \phi_c \\ &= \frac{1}{8\pi} \epsilon^{\mu\nu\rho} \epsilon^{abc} \hat{\phi}_a \partial_\nu \hat{\phi}_b \partial_\rho \hat{\phi}_c, \end{aligned} \quad (39)$$

where $\hat{\phi}_a \equiv \phi_a/\phi$. This is another main result in this paper. The above current density is indeed topological: The total pumped charge is given by the integration of the current density over S^2 embedded in 2+1 dimensions, which is given by the winding number of the Higgs field on S^2 .

To be more specific, let us compute the total current by integrating over $-\infty < x^0 (= t) < \infty$ as well as over C in Fig. 2. To this end, we specify ϕ_a such that

$$\begin{aligned} \phi_1(x) &= \phi_x(x^1) \sin \theta(x^0), \\ \phi_2(x) &= \phi_y(x^2) \sin \theta(x^0), \\ \phi_3(x) &= \phi_0 \cos \theta(x^0), \end{aligned} \quad (40)$$

where $\phi_{x,y}$ is basically the same as Eq. (14), and ϕ_0 is a constant. We further assume the asymptotic behavior of the Higgs field as $|\phi_x(x^1 \rightarrow \pm\infty)| \rightarrow |\phi_0|$ and $|\phi_y(x^2 \rightarrow \pm\infty)| \rightarrow |\phi_0|$ for the spatial part, whereas $\theta(x^0 \rightarrow -\infty) = 0$ and $\theta(x^0 \rightarrow +\infty) = \pi$ for the temporal part. This implies that a trivial system at $t = -\infty$ becomes another trivial system at $t = +\infty$ via the topological state studied in Sec. III.

We compute $j^1(x)$ on C_1 . At $x^1 \rightarrow +\infty$, we have $\phi^2 = \phi_0^2 + \phi_y^2(x^2) \sin^2 \theta(x^0)$. Therefore,

$$\begin{aligned} \langle j^1(x^1 \rightarrow \infty) \rangle &= \frac{2\epsilon^{120} \epsilon^{abc} \phi_a \partial_2 \phi_b \partial_0 \phi_c}{8\pi(\phi_0^2 + \phi_y^2 \sin^2 \theta)^{\frac{3}{2}}} \\ &= -\frac{\phi_x(\infty) \partial_2 \phi_y \sin \theta \partial_0 \theta}{4\pi(\phi_0^2 + \phi_y^2 \sin^2 \theta)^{\frac{3}{2}}}. \end{aligned} \quad (41)$$

Thus, integration over $x^0 (= t)$ gives

$$\begin{aligned} \int_{-\infty}^{\infty} \langle j^1(x^1 = \infty) \rangle dx^0 &= \int_0^\pi \langle j^1(x^1 = \infty) \rangle d\theta \\ &= \frac{-\phi_x(\infty)}{2\pi\phi_0} \frac{\partial_y \phi_y(y)}{\phi_y^2(y) + \phi_0^2}. \end{aligned} \quad (42)$$

Furthermore, the integration of the above on C_1 gives

$$\begin{aligned} \int_{C_1} dx^2 \int_{-\infty}^{\infty} dx^0 \langle j^1(x) \rangle &= \frac{-1}{2\pi} \left[\arctan \frac{\phi_y(\infty)}{\phi_x(\infty)} - \arctan \frac{\phi_y(-\infty)}{\phi_x(-\infty)} \right]. \end{aligned} \quad (43)$$

Together with the contributions on the other lines C_j , the total pumped charge Q is just the index of H in Eq. (29), $|Q| = |\text{ind } H|$, where the sign is generically dependent on the process of the pump. This implies that during the adiabatic change of the ground state between the two trivial ground states with $\phi = (0, 0, \pm\phi_0)$ via topological one with $\phi = (\phi_x, \phi_y, 0)$, the integral charge, just corresponding to the index (or roughly speaking, the number of the zero energy states) of the Hamiltonian with $\phi = (\phi_x, \phi_y, 0)$, flows, which is expected in the topological pump.

V. SUMMARY AND DISCUSSION

In summary, we studied the topological aspects of the Dirac fermion coupled with a two-component Higgs field, which is a naive continuum limit of the BBH lattice model. Since this model has chiral symmetry, we first investigated the zero energy corner states using the index theorem in Sec. III. We argued that a corner can be regarded as a point defect, and hence, the corner states are in the same class of the Jackiw-Rossi states localized at a vortex.

Generically, the Dirac fermion $H = -i\sigma^j \partial_j + \sigma^{d+1} \phi$ in $d = 1, 2$ dimensions is topological [29, 40, 41] in the sense that it has Berry phase $\pm\pi/2$ in $d = 1$ (See Sec. A 4) and Chern number $\pm 1/2$ in $d = 2$. This is why the zero energy state appears in these Dirac fermions. In a similar reason, we can tell that the present Dirac fermion has a corner state because the Higgs field ϕ has nontrivial winding number, as we have shown in this paper.

On the other hand, when we argue the quadrupole phase of the lattice BBH model in terms of the Dirac fermions, we need to take account of the four Dirac

α	(0, 0)	(π , 0)	(0, π)	(π , π)
ϕ_x	$1 + \gamma_x$	$1 - \gamma_x$	$1 + \gamma_x$	$1 - \gamma_x$
ϕ_y	$1 + \gamma_y$	$1 + \gamma_y$	$1 - \gamma_y$	$1 - \gamma_y$

TABLE I: Higgs parameters ϕ_α at four points α . We have set $\lambda_x = \lambda_y = 1$.

fermions derived in Eq. (3). See also Appendix A, where we discuss the same problem for the SSH model. After changing the sign of the two or four Γ matrices associated with $k_j = \pi$ as demonstrated in Eq. (A23), we have

$$H_\alpha = \Gamma^j k_j + \Gamma^{a+2} \phi_{\alpha,a}, \quad (44)$$

where $\alpha = (0, 0), (\pi, 0), (0, \pi), (\pi, \pi)$, and ϕ_α is summarized in Table I, where we have set $\lambda_x = \lambda_y = 1$. From Eq. (29), the topological invariant to characterize each Dirac fermion may be assigned in a similar way demonstrated in Appendix A 4 such that

$$\begin{aligned} Q_\alpha &= \frac{1}{4} \text{sgn} \frac{\phi_{\alpha,y}}{\phi_{\alpha,x}} = \frac{1}{4} (\text{sgn} \phi_{\alpha,x}) (\text{sgn} \phi_{\alpha,y}) \\ &= \frac{q_{\alpha,x}}{\pi} \frac{q_{\alpha,y}}{\pi}, \end{aligned} \quad (45)$$

where q is the Berry phase (with a specific gauge) for one-dimensional Dirac fermion defined in Eq. (A29). According to the same discussion in Eqs. (A3) and (A4), the total topological invariant for the lattice BBH model is the sum of all Q_α ,

$$Q_{\text{BBH}} = \sum_{\alpha} Q_\alpha. \quad (46)$$

Form Table I we arrive at $Q_{\text{BBH}} = 1$ only when $|\gamma_x| < 1 (= \lambda_x)$ and $|\gamma_y| < 1 (= \lambda_y)$.

It should be noted that the Dirac fermion (44) can be characterized by (45) which is given by the Berry phases for x and y directions. Indeed, the lattice BBH model has been characterized by the Wannier-sector polarization [11] or entanglement polarization [25], which are basically Berry phases of the projected one-dimensional model.

As already mentioned, reflection symmetries as well as time reversal symmetry for two-dimensional Dirac model allow just two mass terms, which causes chiral symmetry of the Hamiltonian (4). This enables us to apply the index theorem to the present model, as carried out in Sec. III. Although this is the most general Hamiltonian with reflection symmetries as well as time reversal symmetry, the model can include the chiral symmetry-breaking mass term H_{sb} (13), if time reversal symmetry is relaxed, as discussed in Sec. II C. In what follows, we will mention its effect to the corner states. For the time being, let us consider the case with one corner. With chiral symmetry, the index theorem tells that the Hamiltonian shows at least q zero energy states, when the Higgs field has winding number q . If chiral symmetry is broken but particle-hole

symmetry is unbroken by H_{sb} , the model shows $q \bmod 2$ zero energy states, since the zero energy states protected by chiral symmetry are lifted pairwise to positive and negative energies. Therefore, if q is odd, only one zero energy state is generically protected by particle-hole symmetry for a system with one corner. Thus, we conclude that the zero energy corner states are protected by reflection symmetries.

More generic multi-band systems such as a layered BBH model, reflection symmetries allow various mass terms with broken chiral and particle-hole symmetries with keeping time reversal symmetry. Even in such a case, effective Dirac fermion (4) should appear not necessarily at zero energy, as demonstrated in Appendix A for the SSH model. In a two-leg ladder system introduced in A 3, the edge states appear at nonzero energies as in Eq. (A22). Nevertheless, it is obvious that the edge states can be described by the continuum Dirac fermions (A2). In a three-leg ladder system, the band center is indeed the original SSH model, although the whole system has broken chiral symmetry. Therefore, it is manifest that the edge states in this case are effectively due to the continuum Dirac fermion with chiral symmetry. This feature is also true for the BBH model. Therefore, if we tune the Fermi energy, we see that the corner states, if they exist, are due to those of the Dirac fermion (4), which belongs to the same class of Jackiw-Rossi vortex states.

So far we have discussed the case with only one corner. Let us now consider the system with full open boundary conditions having four corners. In this case, there can appear four corner states. Then, reflection symmetries Eq. (6) ensure that such four corner states are fourfold degenerate. Thus, these states yield the quadrupole charge configuration with an infinitesimal small staggered potential.

This is one of interpretations of the quadrupole phase from the point of view of the continuum Dirac fermion model. In conclusion, the topological origin of the corner states is attributed to the Jackiw-Rossi states of a Dirac fermion in the continuum limit, and their fourfold degeneracy and resultant quadrupole charge configuration in the lattice BBH model are guaranteed by the reflection symmetries.

In Sec. IV, we next introduced a symmetry breaking term and examined the pump, which corresponds to the dipole pump proposed by BBH. We argued that this pump is also topological and the total pumped charge is the same as the index of the Dirac fermion studied in Sec. III.

The dipole pump is realized only if the system has four corners and take the quadrupole charge configuration during the adiabatic pumping process. We just showed that a single Dirac fermion with a point defect (a smooth corner) can yield a topological current. It may be interesting to examine the quadrupole state and the dipole pump in terms of four Dirac fermions mentioned above, preferably taking into account generic BDI symmetry breaking terms.

Acknowledgments

We would like to thank Y. Hatsugai, S. Hayashi, K.-I. Imura, T. Misumi and Y. Yoshimura for fruitful discussions. This work was supported in part by Grants-in-Aid for Scientific Research Numbers 17K05563 and 17H06138 from the Japan Society for the Promotion of Science.

Appendix A: A Dirac fermion description of the SSH model

We present in Appendix A a simple Dirac fermion description of the one-dimensional SSH model, which is helpful in understanding the relationship between the continuum Dirac fermions and the lattice model.

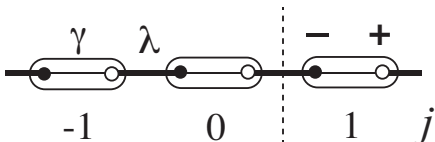


FIG. 3: The SSH model on a one-dimensional lattice. An oval including two sites assigned the chirality $\pm (= -\sigma^3)$ stands for the unit cell. The dotted line stands for the boundary discussed in Sec. A 2.

On a one-dimensional lattice in Fig. 3, the SSH model in the momentum representation is defined by

$$H_{\text{SSH}}(k) = \sigma^2 \lambda \sin k + \sigma^1 (\gamma + \lambda \cos k), \quad (\text{A1})$$

where λ and γ are hopping parameters similar to γ_x and λ_x in Eq. (2), respectively. The crucial symmetry of the model is reflection (inversion) symmetry Eq. (6) implemented by $M_x = \sigma^1$. Since the reflection symmetry prohibits a constant term proportional to σ^3 , the model inevitably has chiral symmetry.

The above Hamiltonian (A1) can be regarded as the Wilson-Dirac Hamiltonian in one dimension, where the first term is the kinetic term and the second term is the mass term with the Wilson term ($\sigma^1 \lambda \cos k$). Therefore, in the continuum limit, we have two fermions near $k = 0$ and $k = \pi$:

$$H_\alpha(k) = \pm \sigma^2 k + \sigma^1 (\gamma \pm 1), \quad \alpha = 0, \pi, \quad (\text{A2})$$

where we have set $\lambda = 1$ for simplicity. This is due to the doubling mechanics [42, 43]. The continuum Hamiltonian also has reflection symmetry as well as chiral symmetry.

The wave function of the ground state is also expanded

around $k \sim 0, \pi$ as

$$\begin{aligned} \psi_j &= \int_{-\pi}^{\pi} \psi(k) e^{ikj} \frac{dk}{2\pi} \\ &\sim \int_{-\Lambda}^{\Lambda} \alpha \psi(k) e^{ikx} \frac{dk}{2\pi} + \int_{-\Lambda}^{\Lambda} \alpha \psi(k + \frac{\pi}{a}) e^{i(k + \frac{\pi}{a})x} \frac{dk}{2\pi} \\ &\rightarrow \int_{-\infty}^{\infty} [\psi_0(k) + e^{i\frac{\pi}{a}x} \psi_\pi(k)] e^{ikx} \frac{dk}{2\pi} \\ &\equiv \psi_0(x) + (-1)^{i\frac{\pi}{a}x} \psi_\pi(x) \equiv \psi(x), \end{aligned} \quad (\text{A3})$$

where $x \sim aj$ with the lattice constant a , $\Lambda \sim \pi/a$ is a cutoff parameter and set $\Lambda \rightarrow \infty$ ($a \rightarrow 0$) in the third line after the linearization of the dispersion, so the $\psi_0(x)$ and $\psi_\pi(x)$ are slowly varying components.

1. Berry phase

As we have mentioned, the SSH model includes two fermions described by the Hamiltonian in Eq. (A2). The wave function of the lattice model can also be approximated by Eq. (A3) including the contribution from two fermions, so the Berry connection reads

$$\begin{aligned} \psi^\dagger \partial_k \psi &\sim \psi_0^\dagger \partial_k \psi_0 + \psi_\pi^\dagger \partial_k \psi_\pi + (\text{osc. terms}) \\ &\equiv A_0(k) + A_\pi(k), \end{aligned} \quad (\text{A4})$$

where the last term is the rapidly oscillating part of the Berry connection including $(-1)^{i\frac{\pi}{a}x}$ which can be neglected. Thus, for the lattice model, the Berry phase could be given by the sum of those of the two Dirac fermions,

$$q_{\text{SSH}} = q_0 + q_\pi. \quad (\text{A5})$$

where

$$q_\alpha = \frac{1}{i} \int_{-\infty}^{\infty} A_\alpha(k) dk. \quad (\text{A6})$$

In what follows, we compute the Berry phases in Eq. (A6). The reflection symmetry of the Hamiltonian (A2)

$$M_x H_\alpha(k) M_x^{-1} = H_\alpha(-k) \quad (\text{A7})$$

allows us to relate the wave functions at $-k$ and k such that

$$\psi_\alpha(-k) = M_x \psi_\alpha(k) e^{i\theta_\alpha(k)}. \quad (\text{A8})$$

This leads to $A_\alpha(-k) = -A_\alpha(k) - i\partial_k \theta_\alpha(k)$. It follows that the Berry phase is given by

$$q_\alpha = \theta_\alpha(0) - \theta_\alpha(\infty). \quad (\text{A9})$$

The phase $\theta_\alpha(k)$ has a constraint at the reflection invariant momentum $k = 0$:

$$p_\alpha e^{i\theta_\alpha(0)} = 1, \quad (\text{A10})$$

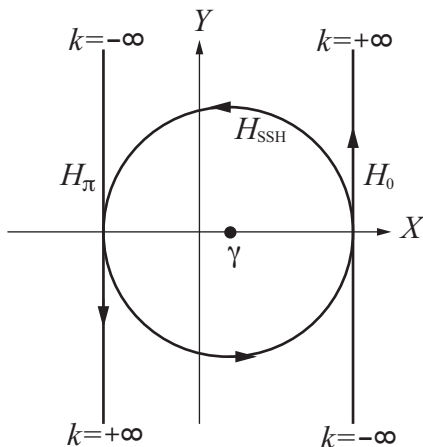


FIG. 4: The integration path for the Berry phase of the SSH model Eq. (A1) (circle) as well as of its continuum limit Eq. (A2) (straight lines). Here, the Hamiltonians Eq. (A1) and Eq. (A2) are parametrized by $H(k) = X(k)\sigma^1 + Y(k)\sigma^2$. The Berry phase is just the winding number of (X, Y) around $X = Y = 0$. The two straight lines can be regarded as a deformation of the circle.

where $p_\alpha = \pm 1$ stands for the parity of the ground state wave function $M_x \psi_\alpha(0) = p_\alpha \psi_\alpha(0)$, i.e., $p_\alpha = -\text{sgn}(\gamma \pm 1)$ for the Hamiltonian Eq. (A2). Thus, we have

$$\theta_\alpha(0) = \pm \frac{1 + \text{sgn}(\gamma \pm 1)}{2} \pi, \quad (\text{A11})$$

where the prefactor \pm in the right-hand side has been introduced for later convenience. It is possible because of $\theta_\alpha(0) = 0, \pm\pi \text{ mod } 2\pi$. On the other hand, the momentum space for the continuum Dirac model (A2) is open at $k = \pm\infty$, there is no constraint on $\theta_\alpha(\infty)$. Thus, the Berry phase (A9) has ambiguity due to $\theta_\alpha(\infty)$.

However, it is noted that from Eq. (A2), $H_0(\pm\infty) = H_\pi(\mp\infty)$ holds. See also Fig. 4. It is thus natural to regard the two straight lines as single points at $k = \pm\infty$, and hence, to choose the wave functions $\psi_0(\pm\infty) = \psi_\pi(\mp\infty)$. Then, the phase $\theta_0(\infty) + \theta_\pi(\infty) = 0 \text{ mod } 2\pi$, and we reach

$$\begin{aligned} q_{\text{SSH}} &= \theta_0(0) + \theta_\pi(0) \\ &= \frac{\pi}{2} [\text{sgn}(\gamma + 1) - \text{sgn}(\gamma - 1)] \\ &= \begin{cases} \pi & (|\gamma| < 1) \\ 0 & (|\gamma| > 1) \end{cases} \text{ mod } 2\pi. \end{aligned} \quad (\text{A12})$$

Therefore, the lattice model has the Berry phase $q_{\text{SSH}} = \pi$ only when $|\gamma| < 1$ ($= |\lambda|$) [44].

2. Edge states

Next, let us discuss the edge states of the model with boundaries described by the Hamiltonian corresponding

to Eq. (A2)

$$H_\alpha(x) = \mp i\sigma^2 \partial_x + \sigma^1(\gamma \pm 1), \quad \alpha = 0, \pi. \quad (\text{A13})$$

As normalizable edge states at $x = 0$, we have the following candidates

$$\psi_{\alpha,-}(x) \propto \begin{pmatrix} e^{\mp(\gamma \pm 1)x} \\ 0 \end{pmatrix}, \quad \psi_{\alpha,+}(x) \propto \begin{pmatrix} 0 \\ e^{\pm(\gamma \pm 1)x} \end{pmatrix}. \quad (\text{A14})$$

The reflection symmetry

$$M_x H_\alpha(x) M_x^{-1} = H_\alpha(-x), \quad (\text{A15})$$

ensures

$$M_x \psi_{\alpha,\mp}(x) = \psi_{\alpha,\pm}(-x). \quad (\text{A16})$$

When $q_{\text{SSH}} = \pi$, the model should show the edge state located at the boundary. Let us examine the edge state from the point of view of the Dirac fermion and its doubler described by H_0 and H_π . To this end, let us cut the one-dimensional chain at the dashed-line in Fig. 3. This is equivalent to imposing the conditions on the wave function of the lattice model, $\psi_{j=1,-} = \psi_{j=0,+} = 0$. According to Eq. (A3), this boundary condition is translated into $\psi_{0,-}(0) - \psi_{\pi,-}(0) = 0$ and $\psi_{0,+}(0) + \psi_{\pi,+}(0) = 0$ in the continuum limit.

Let us first consider the case $|\gamma| < 1$. Both H_0 and H_π allows the zero energy edge states on the $x > 0$ semi-infinite line, so we have

$$\psi_L(x) \sim \alpha \begin{pmatrix} e^{-(\gamma+1)x} \\ 0 \end{pmatrix} + e^{i\frac{\pi}{a}x} \beta \begin{pmatrix} e^{(\gamma-1)x} \\ 0 \end{pmatrix}, \quad (\text{A17})$$

where L means that the state is localized at the left edge $x = 0$ of $x > 0$. Although this state has two independent parameters α and β , the above boundary conditions give one constraint $\alpha - \beta = 0$, and one remaining parameter is determined by the normalization. Thus, only one edge state is allowed. This state has indeed definite chirality.

On the other hand, when $1 < \gamma$, we have the general solution on $x > 0$,

$$\psi_L(x) \sim \alpha \begin{pmatrix} e^{-(\gamma+1)x} \\ 0 \end{pmatrix} + e^{i\frac{\pi}{a}x} \beta \begin{pmatrix} 0 \\ e^{-(\gamma-1)x} \end{pmatrix}. \quad (\text{A18})$$

This also includes two parameters, but the boundary conditions give $\alpha = \beta = 0$. The case $\gamma < -1$ is likewise. Therefore, it turns out that no edge states are allowed for $|\gamma| > 1$. We here conclude that the edge states of the lattice model are actually determined by the combination of those of a Dirac fermion and its doubler (A14).

It should also be noted that in the case $|\gamma| < 1$ the edge state on the other semi-infinite line $x < 0$ is given by

$$\psi_R(x) \sim \alpha \begin{pmatrix} 0 \\ e^{(\gamma+1)x} \end{pmatrix} + \beta e^{i\frac{\pi}{a}x} \begin{pmatrix} 0 \\ e^{(\gamma-1)x} \end{pmatrix}. \quad (\text{A19})$$

The two edge states ψ_L (A17) and ψ_R (A19) are related each other by the reflection symmetry (A15)

$$M_x \psi_L(x) = \psi_R(-x). \quad (\text{A20})$$

Therefore, if the system is defined on a finite chain, e.g., $-\ell < x < \ell$, degenerate edge states are allowed at each edge.

3. Symmetry breaking perturbations

So far we have examined the Dirac fermion with reflection symmetry as well as chiral symmetry. Within two-band system, one may introduce a term such as $H' = \eta\sigma^3 \sin k$ into Eq. (A1) to break chiral symmetry with keeping reflection symmetry. Even in this model, the degenerate zero energy edge states $\psi_{L,R}$ survive due to particle-hole symmetry.

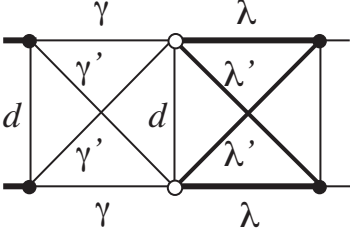


FIG. 5: The 2-leg SSH ladder model which has reflection (inversion) symmetry but broken chiral symmetry.

To demonstrate the model without chiral symmetry and particle-hole symmetry, let us consider a simple ladder generalization of the SSH model illustrated in Fig. 5. The Hamiltonians of 2- and 3-leg ladder system are given by

$$H_{2\text{leg}} = \begin{pmatrix} H_{\text{SSH}} & H'_{\text{SSH}} + d\mathbb{1} \\ H'_{\text{SSH}} + d\mathbb{1} & H_{\text{SSH}} \end{pmatrix},$$

$$H_{3\text{leg}} = \begin{pmatrix} H_{\text{SSH}} & H'_{\text{SSH}} + d\mathbb{1} & 0 \\ H'_{\text{SSH}} + d\mathbb{1} & H_{\text{SSH}} & H'_{\text{SSH}} + d\mathbb{1} \\ 0 & H'_{\text{SSH}} + d\mathbb{1} & H_{\text{SSH}} \end{pmatrix}, \quad (\text{A21})$$

where H_{SSH} and H'_{SSH} are given by Eq. (A1) with intra-chain parameters γ and λ and with inter-chain parameters γ' and λ' , respectively. This ladder model has reflection symmetry implemented by $M_x = \sigma^1 \otimes 1$ but does not have chiral symmetry and particle-hole symmetry.

Suitable change of the basis, the Hamiltonian (A21) can be converted into

$$H_{2\text{leg}} = \text{diag}(H_{\text{SSH}} + H'_{\text{SSH}} + d\mathbb{1}, H_{\text{SSH}} - H'_{\text{SSH}} - d\mathbb{1}),$$

$$H_{3\text{leg}} = \text{diag}(H_{\text{SSH}} + \sqrt{2}(H'_{\text{SSH}} + d\mathbb{1}), H_{\text{SSH}}, H_{\text{SSH}} - \sqrt{2}(H'_{\text{SSH}} + d\mathbb{1})) \quad (\text{A22})$$

Since $H_{\text{SSH}} \pm H'_{\text{SSH}}$ is also the SSH model, it thus turns out that the 2-leg ladder model has edge states when

$|\gamma \pm \gamma'| < |\lambda \pm \lambda'|$ at non-zero energies $E = \pm d$. Interestingly, although the 3-leg ladder model has broken chiral symmetry, the edge states at half-filling is controlled by H_{SSH} . Thus, in the continuum limit of Eq. (A21) or (A22), the ladder Hamiltonian shows several Dirac fermions not necessarily at zero energy. However, these Dirac Hamiltonians should be given by Eq. (A2) locally near the Fermi energy if the system has reflection symmetry, and the 2×2 Dirac fermions with chiral symmetry are responsible for the edge states.

4. A single Dirac fermion

So far we have argued that the doubling of the Dirac fermion gives the correct quantized Berry phase of the SSH model (A12) and corresponding edge states (A17), although the topological property of the edge state of each Dirac fermion (A14) with a sharp boundary is not clear. To reveal this, it may be convenient to introduce smooth boundary connecting different mass parameters at $x = \pm\infty$. In this case, edge states can be regarded as domain wall states to which topological invariant can be assigned.

To demonstrate this, we focus our attention to the topological property of a single Dirac fermion with the mass parameter ϕ , i.e.,

$$H = -i\Gamma^1 \partial_x + \Gamma^2 \phi(x), \quad (\text{A23})$$

where we choose $\Gamma^1 = \sigma^2$, $\Gamma^2 = \sigma^1$, and $\Gamma_5 = -\sigma^3$ for H_0 , and $\Gamma^1 = -\sigma^2$, $\Gamma^2 = -\sigma^1$, and $\Gamma_5 = -\sigma^3$ for H_π in Eq. (A13) to ensure

$$\text{tr} \Gamma_5 \Gamma^1 \Gamma^2 = 2i. \quad (\text{A24})$$

This is the famous Jackiw-Rebbi model [40]. We here assume that ϕ is a smooth function of x , and becomes constant at $x \rightarrow \pm\infty$, $\phi(\pm\infty) = \text{const}$. When $\phi(-\infty) < 0 < \phi(\infty)$, for example, we have the normalizable edge state,

$$\psi_- \propto \begin{pmatrix} e^{-\int^x \phi(x') dx'} \\ 0 \end{pmatrix}, \quad (\text{A25})$$

with chirality $\Gamma_5 = -1$, and hence $n_- = 1$, $n_+ = 0$ and $\text{ind} H = -1$ in Eq. (15). This state is a smooth extension of the edge state $\phi_{0,-}(x)$ in Eq. (A14) towards $x < 0$. Likewise, when $\phi(\infty) < 0 < \phi(-\infty)$, we have $n_- = 0$, $n_+ = 1$ and $\text{ind} H = +1$, and in other cases where $\phi(\pm\infty)$ have the same signs, we have no edge states, and hence $\text{ind} H = 0$.

Because of chiral symmetry, the edge states or domain wall states are at zero energy. In this case, the index theorem clarifies the direct equivalence between the analytical index associated with the zero energy domain wall states and topological index associated with the Berry phase. In this subsection, we briefly investigate the index theorem Eq. (15) for the present Dirac Hamiltonian

(A23). In one dimension, the right-hand side of Eq. (21) is modified into

$$\begin{aligned} \text{ind } H &= -\frac{1}{2} \int \partial_x \langle j_5^1 \rangle dx \\ &= -\frac{1}{2} [\langle j_5^1 \rangle(x = \infty) - \langle j_5^1 \rangle(x = -\infty)]. \end{aligned} \quad (\text{A26})$$

The current $\langle j_5^1 \rangle(x)$ can be calculated in a similar way to Eqs. (23), (24), and (25),

$$\begin{aligned} \langle j_5^1(x) \rangle &= \int \frac{dk}{2\pi} \text{tr}(\Gamma^3) \Gamma^1 \frac{-\Gamma^1(\partial_x + ik) - i\Gamma^2 \phi(x)}{-(\partial_x + ik)^2 + \phi^2 - \sigma^3 \partial_x \phi} \\ &= \int \frac{dk}{2\pi} \frac{2\phi(x)}{k^2 + \phi^2(x)} = \text{sgn } \phi(x), \end{aligned} \quad (\text{A27})$$

We finally obtain the topological index

$$\text{ind } H = -\frac{1}{2} [\text{sgn } \phi(\infty) - \text{sgn } \phi(-\infty)], \quad (\text{A28})$$

which is exactly the same as the analytical index mentioned above. Note that this result is nothing to do with

specific choices of the Γ -matrices in Eq. (A23): Only the anti-commutation relation between Γ -matrices and the normalization in Eq. (A24) are responsible for Eqs. (A27) and (A28). Since the index of H may be given by the topological numbers, we assume

$$\text{ind } H = -[q(\infty) - q(-\infty)]/\pi. \quad (\text{A29})$$

Then, we have $q(\pm\infty) = \frac{\pi}{2} \text{sgn } \phi(\pm\infty)$ apart from a constant. Thus, for the fermion with a constant mass m , $H = -i\Gamma^1 \partial_x + \Gamma^2 m$, it is reasonable to assign the topological number $q = \frac{\pi}{2} \text{sgn } m$. This is nothing but the Berry phase with a special choice of gauge. With the definition of the Γ -matrices in Eq. (A23) for H_α , the masses are $1 + \gamma$ and $1 - \gamma$ for $\alpha = 0$ and $\alpha = \pi$, respectively. This leads to $q_0 = \frac{\pi}{2} \text{sgn}(1 + \gamma)$ and $q_\pi = \frac{\pi}{2} \text{sgn}(1 - \gamma)$, which indeed reproduces Eq. (A12). Uncertain constant terms vanish if the Dirac fermions and its doublers are combined.

-
- [1] Y. Hatsugai, *Physical Review Letters* **71**, 3697 (1993).
[2] C. L. Kane and E. J. Mele, *Physical Review Letters* **95**, 226801 (2005).
[3] C. L. Kane and E. J. Mele, *Physical Review Letters* **95**, 146802 (2005).
[4] X.-L. Qi, T. L. Hughes, and S.-C. Zhang, *Physical Review B* **78**, 195424 (2008).
[5] M. Z. Hasan and C. L. Kane, *Reviews of Modern Physics* **82**, 3045 (2010).
[6] X.-L. Qi and S.-C. Zhang, *Reviews of Modern Physics* **83**, 1057 (2011).
[7] S. Murakami, *New Journal of Physics* **9**, 356 (2007).
[8] A. Burkov and L. Balents, *Phys. Rev. Lett.* **107**, 127205 (2011).
[9] X. Wan, A. M. Turner, A. Vishwanath, and S. Y. Savrasov, *Physical Review B* **83**, 205101 (2011).
[10] W. A. Benalcazar, B. A. Bernevig, and T. L. Hughes, *Science* **357**, 61 (2017).
[11] W. A. Benalcazar, B. A. Bernevig, and T. L. Hughes, *Physical Review B* **96**, 245115 (2017).
[12] F. Liu and K. Wakabayashi, *Physical Review Letters* **118**, 076803 (2017).
[13] S. Hayashi (2016), arXiv:1611.09680.
[14] J. Langbehn, Y. Peng, L. Trifunovic, F. von Oppen, and P. W. Brouwer, *Physical Review Letters* **119**, 246401 (2017).
[15] Z. Song, Z. Fang, and C. Fang, *Physical Review Letters* **119**, 246402 (2017).
[16] K. Hashimoto, X. Wu, and T. Kimura, *Physical Review B* **95**, 165443 (2017).
[17] M. Ezawa, *Physical Review Letters* **120**, 026801 (2018).
[18] M. Ezawa (2018), arXiv:1801.00437.
[19] F. Schindler, A. M. Cook, M. G. Vergniory, Z. Wang, S. S. P. Parkin, B. A. Bernevig, and T. Neupert, *Science Advances* **4** (2018).
[20] S. Imhof, C. Berger, F. Bayer, J. Brehm, L. Molenkamp, T. Kiessling, F. Schindler, C. H. Lee, M. Greiter, T. Neupert, et al. (2017), arXiv:1708.03647.
[21] E. Khalaf, *Physical Review B* **97**, 205136 (2018).
[22] Y. Wang, M. Lin, and T. L. Hughes (2018), arXiv:1804.01531.
[23] A. Matsugatani and H. Watanabe (2018), arXiv:1804.02794.
[24] L. Trifunovic and P. Brouwer (2018), arXiv:1805.02598.
[25] T. Fukui and Y. Hatsugai (2018), arXiv:1805.02831.
[26] T. Misumi, *Journal of High Energy Physics* **2013**, 63 (2013).
[27] A. Altland and M. R. Zirnbauer, *Physical Review B* **55**, 1142 (1997).
[28] A. P. Schnyder, S. Ryu, A. Furusaki, and A. W. W. Ludwig, *Physical Review B* **78**, 195125 (2008).
[29] R. Jackiw and P. Rossi, *Nucl. Phys. B* **190** (1981).
[30] J. C. Y. Teo and C. L. Kane, *Physical Review B* **82** (2010).
[31] W. P. Su, J. R. Schrieffer, and A. J. Heeger, *Physical Review Letters* **42**, 1698 (1979).
[32] C. Callias, *Commun. Math. Phys.* **62**, 213 (1978).
[33] E. J. Weinberg, *Physical Review D* **24** (1981).
[34] A. J. Niemi and G. W. Semenoff, *Physical Review D* **30**, 809 (1984).
[35] A. J. Niemi and G. W. Semenoff, *Phys. Rep.* **135**, 99 (1986).
[36] T. Fukui and T. Fujiwara, *Journal of the Physical Society of Japan* **79**, 033701 (2010).
[37] T. Fujiwara and T. Fukui, *Physical Review D* **85**, 125034 (2012).
[38] K. Shiozaki, T. Fukui, and S. Fujimoto, *Physical Review B* **86**, 125405 (2012).
[39] T. Fukui and T. Fujiwara, *Physical Review B* **96**, 205404 (2017).

- [40] R. Jackiw and C. Rebbi, *Physical Review D* **13** (1976).
- [41] J. Goldstone and F. Wilczek, *Physical Review Letters* **47**, 986 (1981).
- [42] H. B. Nielsen and M. Ninomiya, *Nuclear Physics B* **185**, 20 (1981).
- [43] H. B. Nielsen and M. Ninomiya, *Nuclear Physics B* **193**, 173 (1981).
- [44] S. Ryu and Y. Hatsugai, *Physical Review Letters* **89**, 077002 (2002).